Available online at www.sciencedirect.com
SCIENCE DIRECT®
Thermochimica Acta 426 (2005) 157–161
thermochimica acta
www.elsevier.com/locate/tca

DSC studies on crystallization mechanisms of tellurite glasses☆

K. Yukimitu[a], R.C. Oliveira[a], E.B. Araújo[a,*], J.C.S. Moraes[a], L.H. Avanci[b]

[a] *Departamento de Física e Química, Universidade Estadual Paulista, Grupo Vidros e Cerâmicas, Caixa Postal 31, 15385-000 Ilha Solteira, SP, Brazil*
[b] *Departamento de Física Aplicada, Instituto de Física, Universidade de São Paulo, 05508-900 São Paulo, SP, Brazil*

Received 22 April 2004; received in revised form 30 June 2004; accepted 29 July 2004
Available online 11 September 2004

Abstract

The purpose of this work is to study the $20Li_2O–80TeO_2$ glass using the differential scanning calorimetry (DSC) and X-ray diffraction (XRD) techniques in order to understand the crystallization kinetics on this glass matrix. To study the glass by DSC, screened samples with different particle sizes to resolve the observed asymmetrical crystallization peak were used. DSC curves for particles smaller than 38 μm in size show two distinct crystallization peaks, associated to distinct phase transformation in this glass, leading to activation energies at 301 and 488 kJ mol^{-1}. XRD analysis reveals that the first crystallization peak is attributed to TeO_2 crystalline phase while the second one to the α-TeO_3 and an unidentified phase.
© 2004 Elsevier B.V. All rights reserved.

Keywords: DSC; Crystallization mechanism; Tellurite glasses

1. Introduction

TeO_2-based glasses were most studied in the last 10 years, considering the scientific and technological interest due to their high refractive indices, low melting temperatures, high dielectric constants and good infrared transmissions [1]. Tellurite glass may be formed from different systems including phosphate, borate and others [2]. The main studies on TeO_2-based glasses were centered on optical properties with special attention in using these vitreous systems as nonlinear optical glasses for second (χ^2) and third harmonic (χ^3) generation [3,4]. An important tellurite system is formed using Li_2O as a network modifier to produce $Li_2O–TeO_2$ glasses. In literature, these $Li_2O–TeO_2$ glasses are known for their excellent nonlinear optical properties and depending on composition presents a χ^3 almost one order greater than some other important oxide glasses [4]. However, structural [5–7] and electrical properties [8] have been investigated in order to understand all aspects of these glasses.

Parallel to the optical property investigations, there is a crescent interest for the fabrication of transparent oxide glasses containing specific microcrystallites in the matrix glass: the glass-ceramics. Optical properties of TeO_2-based glass-ceramic containing specific microcrystallites are very interesting and might be probable as new optical glasses [9,10]. On the other hand, the glass-ceramics fabrication requires ability and knowledge to control the nucleation and crystallization processes of different vitreous matrices. Consequently, it is important to know the physical and thermal characteristics of interest, particularly if the glass is to be applied in a specific technological area. Knowledge of the nucleation rate as a function of temperature is essential for predicting phase formation and microstructures in modern materials development.

The purpose of this work is to study the crystallization kinetic on $20Li_2O–80TeO_2$ glass for glass-ceramic fabrication from this important matrix glass. For this purpose, X-ray diffraction analysis (XRD) and differential scanning

☆ Authors are also members of the Centro Virtual de Pesquisa em Materiais (CVMat), UNESP center for Materials Science Research.

* Corresponding author. Tel.: +55 18 3743 1029; fax: +55 18 3742 4868.
E-mail address: eudes@fqm.feis.unesp.br (E.B. Araújo).

0040-6031/$ – see front matter © 2004 Elsevier B.V. All rights reserved.
doi:10.1016/j.tca.2004.07.016

calorimetry (DSC) were used as combined techniques to understand and control the crystallization on this glass.

2. Experimental

The $20Li_2O$–$80TeO_2$ glass examined in this work was prepared using the conventional melt quenching method starting from commercial powder reagents Li_2CO_3 (Alfa Aesar, 99%) and TeO_2 (Alfa Aesar, 99.95%). After mixed in appropriate proportions, using a 15 g batch weight, powder was melted using a platinum crucible at 900 °C for 30 min in an electric furnace. The melt obtained was poured into a mould and a transparent pale yellow sample with 8 mm thickness was obtained. The structure of the crystallized phases observed in powdered glasses after different annealing treatments were analyzed by XRD using Cu Kα radiation in a Rigaku Rotaflex RU200B equipment with a rotating anode.

Using a TA instrument – DSC 2920 (temperature accuracy of ± 0.1 °C) – DSC measurements were performed to study the thermal properties of the studied glass as a function of the particle size. The as-quenched glass was ground and screened to five different particle-size intervals: less than 38, 45–38, 63–45 and 75–63 μm. Each fraction was used for DSC measurements, which were carried out using a constant sample weight of 20 mg, in aluminum pans under a flowing (50 $cm^3\,min^{-1}$) atmosphere of dry nitrogen, at 10 °C min^{-1} controlled heating rate.

To determine activation energy (E) for the crystallization, different particle size glasses were crystallized at four heating rates, ϕ (2.5, 5.0, 7.5 and 10.0 °C min^{-1}). The data were analyzed using the Kissinger equation [11],

$$\ln\left(\frac{T_p^2}{\phi}\right) = \frac{E}{RT_p} + \text{constant} \quad (1)$$

where T_p is a temperature corresponding to the maximum of the DSC crystallization peak and R is the gas constant. The activation energy was calculated from the slopes of the linear fits to the experimental data from a plot of $\ln(T_p^2/\phi)$ versus $1/T_p$ for different particle size.

3. Results and discussion

The glass transition temperature (T_g), crystallization temperature (T_x), crystallization peak temperature (T_p) and melting temperature (T_m) were determined from DSC measurements as indicated in Fig. 1. Inset in this figure shows details to determine onset temperature T_g. As the studies in this work were centered on crystallization process, only T_g, T_x and T_p were summarized in Table 1 as a function of particle size. As we can see in this table, the thermal parameters are influenced differently by the particle size. As expected, T_g presents essentially the same value at around 536 K for different particle size but T_x shifts slightly from 621 to 609 K when particle size decreases from 63–75 μm to less than 38 μm. Similar behavior was also observed in T_p, which shifts from 632 to 622 K when particle size decreases. This fact may be associated with particle size effects on heat transfer. Considering a given heating rate, larger particles would have greater heat transfer resistance, during DSC scan, when compared with small particles. Afterwards, the shift on crystallization peak results was observed. In Table 1, an additional crystallization peak at 626 K was also introduced, observed at particle size smaller than 38 μm. Details will be discussed further on in this work. The thermal stabilities, qualitatively determined from ΔT in Table 1, decrease for small particle size. It is understood that volume decreases for small particle size while the superficial area increases.

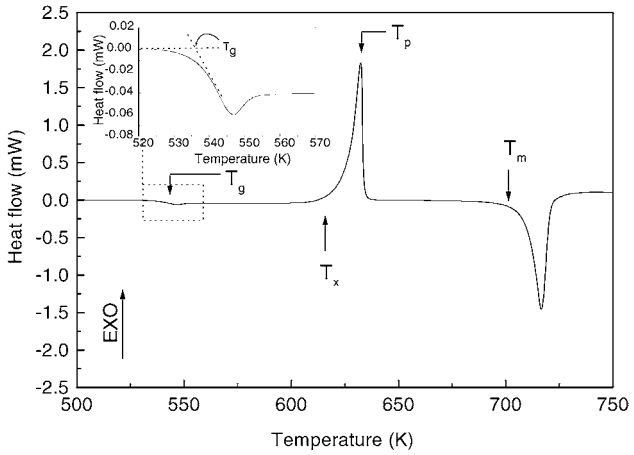

Fig. 1. DSC curve for the as-quenched $20Li_2O$–$80TeO_2$ glass (recorded at a heating rate of 10 K min^{-1}). In this figure are indicated the glass transition temperature (T_g), the crystallization temperature (T_x), the peak crystallization temperature (T_p) and the melting temperature (T_m).

Frequently, DSC measurements are performed on powders and as a result, the interpretation of kinetic crystallization in glasses requires some care as possible particle size effects on the crystallization are present. Fig. 2 shows DSC crystallization peaks as a function of the temperature, performed for different heating rate (ϕ) and particle size. The use of different heating rates leads to activation energy calculus from Eq. (1) and show up like different crystallization processes responsible for the observed asymmetry in DSC peaks for the following particle size: 63–75, 45–63 and 38–45 μm. In most fine powdered glass, particle size smaller than 38 μm, this asymmetry became evident as indicated by one peak at

Table 1
Summary for physical parameters of $20Li_2O$–$80TeO_2$ glasses as a function of particle size

Particle size (μm)	T_g (K)	T_x (K)	$\Delta T = T_x - T_g$	T_p (K)	E (kJ mol^{-1})
63–75	537	621	84	632	254
45–63	537	618	81	630	248
38–45	536	614	78	629	237
<38	536	609	73	622 and 626	301 and 488

Parameters are shown for ϕ = 10 K min^{-1} heating rate.

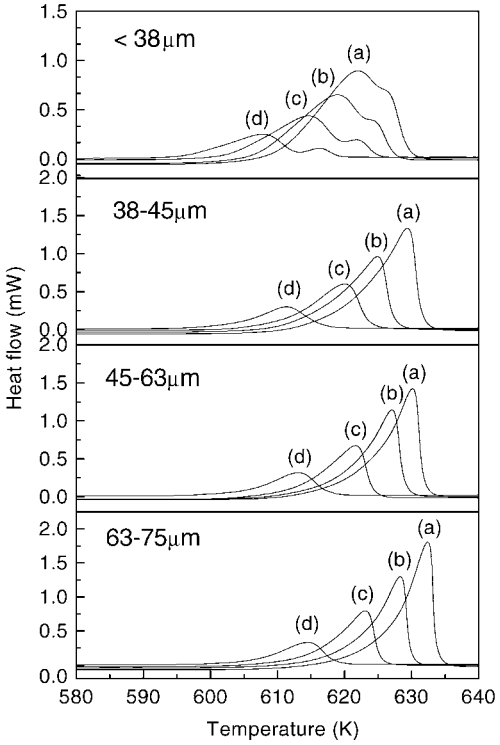

Fig. 2. DSC curves for $20Li_2O$–$80TeO_2$ glasses as a function of particle size, which were recorded at 10 K min^{-1} (a), 7.5 K min^{-1} (b), 5.0 K min^{-1} (c) and 2.5 K min^{-1} (d) heating rates.

around 622 K and a shoulder close to 626 K (see DSC curve recorded at 10 K min^{-1} in Fig. 2). Decreasing the heating rate to 2.5 K min^{-1}, this shoulder splits into two crystallization peaks at 608 and 616 K. As observed in this figure, the combination particle size and heating rate evidenced at least two distinct phase crystallizations.

Fig. 3 shows plots of $\ln(T_p^2/\phi)$ *versus* $1/T_p$ for glass powder samples with different particle size. As described before, the activation energy was calculated from linear fits to the experimental data using the Eq. (1). Calculated values for

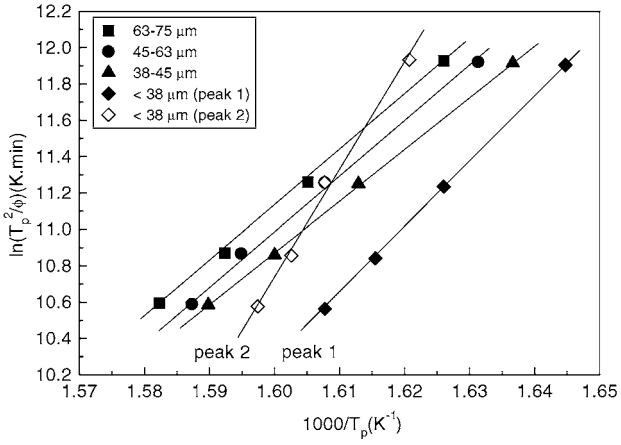

Fig. 3. Kissinger plots for the crystallization peaks in $20Li_2O$–$80TeO_2$ glasses as a function of particle size.

different particle sizes were also summarized in Table 1. In this table, we observe that activation energy decreases from 254 to 237 kJ mol^{-1} when particle size decreases from 63–75 to 38–45 μm whereas for particle size smaller than 38 μm it was possible to calculate two distinct activation energies at 301 and 488 kJ mol^{-1}. This implies that in this glass system there are distinct phase transformations with distinct energies, only evidenced by DSC at smallest particle size. In addition, the activation energies obtained in this work are very close to those reported in the literature for $30Li_2O$–$70TeO_2$ glass, which in contrast with the $20Li_2O$–$80TeO_2$ composition exhibits in bulk form two distinct crystallization peaks [5,6].

In Fig. 2 the presence of a well-defined couple of crystallization peaks for small particle size (size < 38 μm) is a strong indicative of distinct phase transformations on glass but to confirm this additional information with another experimental technique is necessary (XRD), as will be described below. In this work, different crystallization mechanisms, such as superficial or volumetric processes, were not considered. In practice, superficial crystallization is difficult to avoid and it is questionable if only the volume crystallization occurs. In fact, the surface nucleation and crystallization depends on several factors such as surface quality, cracks, elastic stress and others [12]. Traditional method, which includes isotherm process and microscopy analysis [13], is a good way to study surface and volume nucleation and crystallization in glasses but the involved mechanisms are still not completely understood. On the other hand, combined DSC and XRD results obtained in the present work suggest that crystallization can be essentially attributed to a distinct phase transformation.

In order to clarify the true reason why a shoulder appears on glass with small particle size (see grain < 38 μm in Fig. 2), suggesting a possible distinct phase crystallization, several glass powders were heat thermal annealed at different temperatures to induce the nucleation and a selective crystallization on glass. Fig. 4 shows XRD patterns of as-quenched glasses and heat annealed between 310 and 360 °C in electric

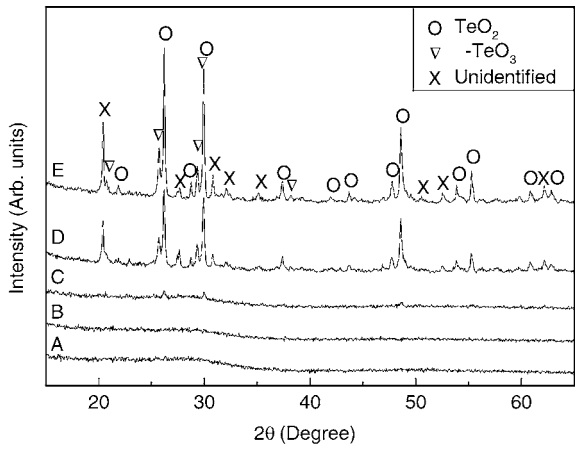

Fig. 4. X-ray diffraction patterns of $20Li_2O$–$80TeO_2$ glasses as-quenched (A), and previously heat annealed at 310 °C (B), 330 °C (C), 350 °C (D) and 360 °C (E) for 5 min.

furnace for 5 min. As we can see, the as-quenched and heat annealed glass at 310 °C shows a typical amorphous characteristics. However, the glass state tends to disappear resulting in a glass-ceramic when the glass is heat annealed at higher temperatures. In glass annealed at 330 °C, some crystallization peaks appear for 2θ at around 26.2°, 29.9° and 48.6°, which were attributed to TeO_2 crystalline phase permeating glass matrix. Increasing the annealing temperature to 350 and 360 °C an unidentified phase and α-TeO_3 crystalline phase appears and coexists with the TeO_2 phase, as indicated by indexed peaks in Fig. 4E.

Using the (1 1 0), (1 1 1), (1 0 2), (2 0 0) and (2 1 2) *hkl* planes of the XRD pattern in Fig. 4E, respectively, observed at 26.19°, 28.74°, 29.94°, 37.39° and 48.59°, the lattice constants a and c for TeO_2 tetragonal phase were calculated as a = 4.811 Å and b = 7.618 Å. These lattice parameters agree with JCPDS (42-1365) data card, confirming the TeO_2 phase crystallization. These results suggest a hierarchy on this glass crystallization and the TeO_2 phase crystallization occurs prior to α-TeO_3 and an unidentified phase. It is interesting to observe that an expected lithium tellurite phase was not properly identified in Fig. 4. Several possibilities were tried including the $LiTeO_3$ or Li_2TeO_3 phases in our XRD refinements but these attempts were frustrated. In another $30Li_2O$–$70TeO_2$ glass matrix, whose crystallization was studied using different techniques such as DSC and X-ray diffraction [6], an unidentified phase was also observed but this crystalline phase converts to α-$Li_2Te_2O_5$ at high annealing temperatures. On the other hand, the present result for the studied glass composition disagrees if compared with previous studies [5,6]. A possible explanation may be founded if we consider that $30Li_2O$–$70TeO_2$ composition is a eutectic point on the phase diagram of the pseudo-binary Li_2O–TeO_2 system [5]. Thus, based on this phase diagram and the $20Li_2O$–$80TeO_2$ glass composition, the unidentified phase in the present work is most probably a kind of crystalline lithium–tellurium phase.

Kinetic studies are often performed by monitoring changes in a specific physical parameter during crystallization. Studies using non-isothermal data are frequently interpreted erroneously as possible finite size effects on crystallization kinetics are neglected. These effects on the crystallization kinetics have been considered by experimental [14] and theoretical [15,16] studies and the interpretations of the present work were based on the studies by these researchers. Thus, considering particle size effects on DSC crystallization peak (Fig. 2) it was possible to arrive at an interpretation regarding the two distinct phase transformations. With respect to the hierarchy on crystallization of the $20Li_2O$–$80TeO_2$ glass, some studies were carried out on similar matrix but this hierarchy was not previously predicted. Using differential thermal analysis (DTA), early studies to construct the phase diagram of the pseudo binary system Li_2O:TeO_2 indicated a eutectic point to a $30Li_2O$–$70TeO_2$ composition and a metastable phase could be observed when this glass was heat annealed at 410 °C [5]. In this work, the observed metastable phase was identified as a monoclinic phase permeating the $30Li_2O$–$70TeO_2$ glass matrix and can be interpreted as a "link" between the unidentified phase and the orthorhombic phase, this last one crystallized at high heat annealing.

The $30Li_2O$–$70TeO_2$ glass crystallization was also studied from DSC and X-ray diffraction more recently [7]. In this work, an unidentified phase was also observed and this crystalline phase converts to α-$Li_2Te_2O_5$ while the vitreous TeO_2 phase is clearly converted to α-TeO_2 crystalline phase [7]. Apparently, there are contradictions between these both cited works with respect to crystallization in the $30Li_2O$–$70TeO_2$ glass matrix. However, the crystallization mechanisms in these Li_2O–TeO_2 glasses are not completely understood and must be investigated in detail. In contrast with these works in $30Li_2O$–$70TeO_2$ glass, the hierarchy on crystallization was evident in our studied $20Li_2O$–$80TeO_2$ glass, the metastable phase was not observed and the unidentified phase could not be systematically identified up to this moment.

4. Conclusion

The crystallization kinetic on the $20Li_2O$–$80TeO_2$ glass was studied by simultaneously using XRD and DSC techniques to understand the glass-ceramic formation from this glass. A detailed DSC analysis as a function of different particle sizes was possible to predict a phase transformation on this glass. Finally, the XRD analysis revealed a crystallization hierarchy on this glass, starting with the TeO_2 crystalline phase permeating the glass matrix followed by the simultaneous crystallization of the α-TeO_3 and an unidentified phase, leading to two distinct activation energies at 301 and 488 kJ mol^{-1}, respectively.

Acknowledgements

We would like thank Conselho Nacional de Desenvolvimento Científico e Tecnológico (CNPq), Coordenação de Aperfeiçoamento de Pessoal de Nível Superior (CAPES) and Fundação de Amparo à Pesquisa do Estado de São Paulo (FAPESP) for financial support.

References

[1] A.K. Yakhkind, J. Am. Ceram. Soc. 49 (1966) 670.
[2] V. Kozhukharov, M. Marinov, I. Gugov, H. Bürger, W. Vogel, J. Mater. Sci. 18 (1983) 1557–1563.
[3] K. Tanaka, K. Kashima, K. Hirao, N. Soga, A. Mito, H. Nasu, J. Non-cryst. Solids 185 (1995) 123–126.
[4] H. Nasu, O. Matsushita, K. Kamiya, H. Kobayashi, K. Kubodera, J. Non-cryst. Solids 124 (1990) 275–277.
[5] P. Balaya, C.S. Sunandana, J. Non-cryst. Solids 162 (1993) 253–262.
[6] I. Avramov, G. Guinev, A.C.M. Rodrigues, J. Non-cryst. Solids 271 (2000) 12–17.

[7] T. Taniguchi, S. Inoue, T. Mitsuhashi, A. Nukai, J. Appl. Cryst. 33 (2000) 64–67.
[8] R.A. Montani, M. Lévy, J.L. Souquet, J. Non-cryst. Solids 149 (1992) 249–256.
[9] T. Komatsu, H. Tawarayama, K. Matusita, J. Ceram. Soc. Jpn. 101 (1993) 48–52.
[10] K. Shioya, T. Komatsu, H.G. Kim, R. Sato, K. Matusita, J. Non-cryst. Solids 189 (1995) 16–24.
[11] H.E. Kissinger, J. Res. Natl. Bur. Stand. 57 (1956) 217–221.
[12] E.D. Zanotto, V.M. Fokin, Philos. T. Roy. Soc. A 361 (2003) 591–612.
[13] R. Müller, E.D. Zanotto, V.M. Fokin, J. Non-cryst. Solids 274 (2000) 208–231.
[14] C.S. Ray, D.E. Day, J. Am. Ceram. Soc. 73 (1990) 439–442.
[15] K.F. Kelton, K.L. Narayan, L.E. Levine, T.C. Cull, C.S. Ray, J. Non-cryst. Solids 204 (1996) 13–31.
[16] K.F. Kelton, Mat. Sci. Eng. A 226–228 (1997) 142–150.